

PAPER • OPEN ACCESS

Multilayered polycrystallization in single-crystal YSZ by laser-shock compression

To cite this article: Yasuhiko Nishimura *et al* 2015 *J. Phys. D: Appl. Phys.* **48** 325305

View the [article online](#) for updates and enhancements.

Related content

- [Femtosecond laser-driven shock-induced dislocation structures in iron](#)
Tomoki Matsuda, Tomokazu Sano, Kazuto Arakawa *et al.*
- [Femtosecond laser induced nanostructuring of zirconium in liquid confined environment](#)
Nisar Ali, Shazia Bashir, Umm-i-Kalsoom *et al.*
- [Analysis of laser shock waves and resulting surface deformations in an Al-Cu-Li aluminum alloy](#)
P Peyre, L Berthe, V Vignal *et al.*

Recent citations

- [Modification of single-crystalline yttria-stabilised zirconia induced by radiation heating from laser-produced plasma](#)
Yoshitaka Mori *et al*
- [Characterizing near-surface firn using the scattered signal component of the glacier surface return from airborne radio-echo sounding](#)
Anja Rutishauser *et al*
- [Amorphous nanostructuralization in HOPG by \$10^{14}\$ W cm⁻² laser](#)
Yasuhiko NISHIMURA *et al*



IOP | ebooks™

Bringing you innovative digital publishing with leading voices to create your essential collection of books in STEM research.

Start exploring the collection - download the first chapter of every title for free.

Multilayered polycrystallization in single-crystal YSZ by laser-shock compression

Yasuhiko Nishimura^{1,2}, Yoneyoshi Kitagawa¹, Yoshitaka Mori¹,
Tatsumi Hioki³, Hirozumi Azuma³, Tomoyoshi Motohiro³, Osamu Komeda⁴,
Katsuhiko Ishii¹, Ryohei Hanayama¹, Takashi Sekine⁵, Atsushi Sunahara⁶,
Tsutomu Kajino³, Teppei Nishi³, Takuya Kondo⁴, Manabu Fujine⁴,
Nakahiro Sato⁵, Takashi Kurita⁵, Toshiyuki Kawashima⁵, Hirofumi Kan⁵,
Eisuke Miura⁷ and Yasuhiko Sentoku⁸

¹ The Graduate School for the Creation of New Photonics Industries, 1955-1 Kurematsu-cho, Nishi-ku, Hamamatsu, Shizuoka 431-1202, Japan

² Toyota Technical Development Corporation, 1-21 Imae, Hanamoto-cho, Toyota, Aichi 470-0334, Japan

³ Toyota Central Research and Development Laboratories, Inc., 41-1 Yokomichi, Nagakute, Aichi 480-1192, Japan

⁴ Toyota Motor Corporation, 1200 Mishuku, Susono, Shizuoka 410-1193, Japan

⁵ Hamamatsu Photonics K.K., 1820 Kurematsu-cho, Nishi-ku, Hamamatsu, Shizuoka 431-1202, Japan

⁶ Institute for Laser Technology, 1-8-4 Utsubo-honmachi, Nishi-ku, Osaka 550-0004, Japan

⁷ The National Institute of Advanced Industrial Science and Technology, 1-1-1 Umezono, Tsukuba, Ibaraki 305-8568, Japan

⁸ Department of Physics, University of Nevada, Reno 1664 N Virginia Street, Reno, NV 89557, USA

E-mail: yasuhiko2460@gpi.ac.jp

Received 12 March 2015, revised 14 May 2015

Accepted for publication 9 June 2015

Published 13 July 2015



Abstract

A single shot of an ultra-intense laser with 0.8 J of energy and a pulse width of 110 fs (peak intensity of $1.15 \times 10^{17} \text{ W cm}^{-2}$) is divided into two beams and the two beams counter-irradiated onto a 0.5 mm-thick single crystal yttria-stabilized zirconia (YSZ), changing the YSZ into a multilayered polycrystalline state. The laser-driven shock wave of the intensity $\sim 7.6 \times 10^{12} \text{ Pa}$ penetrated the crystal as deep as 96 μm , causing formation of a four-layered structure (the first layer from the surface to 12 μm , the second from 12 to 28 μm , the third from 28 to 96 μm , and the fourth from 96 to 130 μm , respectively). The grain size of the first layer was 1 μm , while that of the second layer was broken into a few tens nanometers. The grain size of the third layer was a few hundred nanometers to a few ten micrometers. The area deeper than 96 μm remained as a single crystal. The plasma heat wave might remelt the first layer, resulting in the grain size becoming larger than that of the second layer. The surface polycrystallization seems to maintain the residual stresses frozen in the film thickness direction. Our experimentally observed spatial profile of the grain size can be explained by this shock and heat waves model.

Keywords: laser-shock compression, polycrystallization, ultra-intense laser

(Some figures may appear in colour only in the online journal)



Content from this work may be used under the terms of the [Creative Commons Attribution 3.0 licence](https://creativecommons.org/licenses/by/3.0/). Any

further distribution of this work must maintain attribution to the author(s) and the title of the work, journal citation and DOI.

1. Introduction

Barium titanate, ferrite, and zirconia are typical fine ceramics with useful dielectric, magnetic, and mechanical properties,

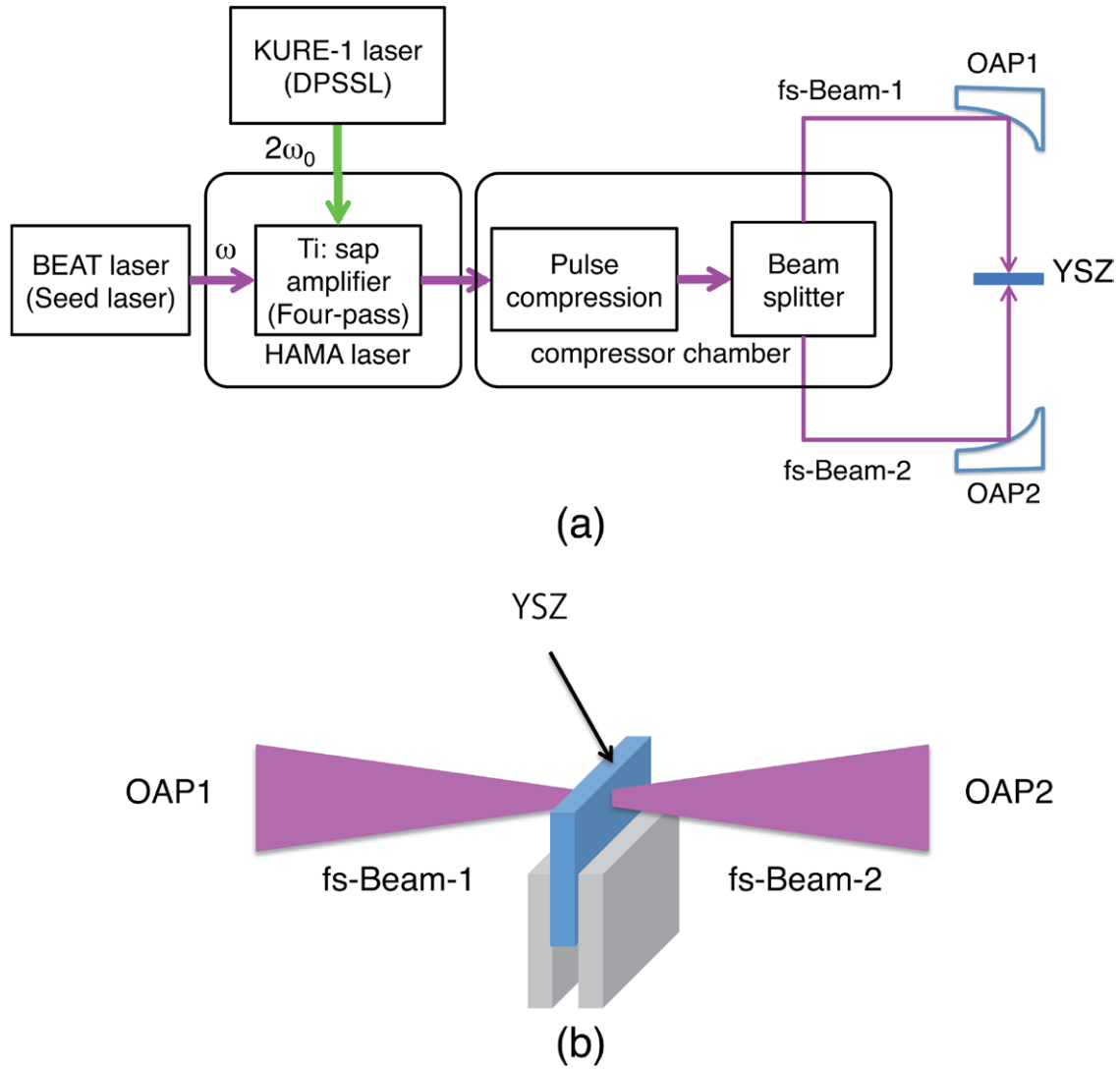


Figure 1. (a) Laser block-diagram; $2\omega_0 = 527$ nm and $\omega = 810$ nm. OAP 1 and OAP 2 are off-axial parabolic mirrors. (b) Irradiation layout on the YSZ.

and are widely used in various industries. Ytria-stabilized zirconia (YSZ), in particular, is used in fuel-cells and the oxygen sensors of motor cars because of its high ion conduction that is suitable for solid electrolytes at a high temperature [1, 2]. However, ceramics are brittle and easily destroyed by impact or thermal shock. If nanocrystallization overcomes such defects and increases the toughness of ceramics with respect to fracture, ceramics could be used much more widely in industries. In this paper, we demonstrate that a single shot of an ultra-intense laser nanocrystallizes the ceramics. Our results have three characteristic points:

1. Single shot results on ceramics at the laser intensity of 1×10^{17} W cm⁻².
2. Production of a multilayered polycrystalline, and the nanocrystalline from a single crystal YSZ ceramics.
3. A residual stress remaining more than 100 days.

Recently, the phase transitions of materials using a femtosecond laser have been reported [3–9]. Shock compression with a femtosecond laser is a formed high energy

Table 1. Experimental parameters of the irradiated ultra-intense laser.

Energy [J]	0.42 (1 Beam)
Pulse width [fs]	110
Beam spot size [μ m]	65
Wavelength [μ m]	0.81
Peak intensity [W cm ⁻²]	1.15×10^{17}

density state in the material without a temperature rise [3]. They have observed the metals, not ceramics. Tsujino *et al* [4, 5] reported that a lot of defects inside the silicon happen by femtosecond laser of 1×10^{16} W cm⁻², and that plastic deformation happens. They have not observed the phenomena either, as for the 2nd or the 3rd of our results. Matsuda *et al* [6, 7] reported that the ablation pressure was ~ 1 TPa by multiple shots of sub-mJ femtosecond laser-driven shock pulse and that the coarse crystalline iron grains were changed into nanocrystals characterized by the high density of dislocations in a depth of 2 μ m from the surface. Their

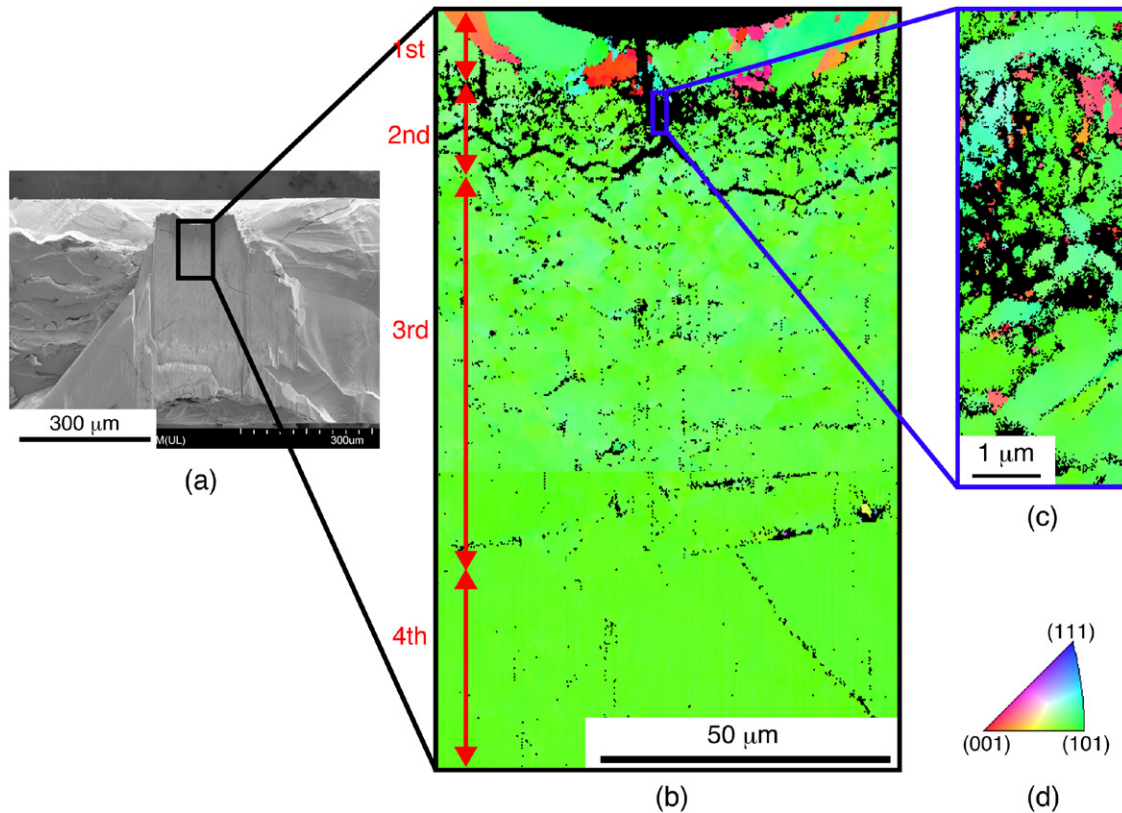


Figure 2. (a) Cross-section SEM image. (b) EBSD analysis area; depth $130\ \mu\text{m}$, width $80\ \mu\text{m}$. This figure shows four layers, designated as first, second, third, and fourth. (c) Expanded view of the blue square of (b). The area that appears black in (b) has a few tens nm grains. (d) Crystal orientation patterns.

results are similar to our 2nd result. But they have not observed either the 1st or the 3rd of our results. Sano *et al* [8, 9] reported that a hexagonal crystal diamond is generated in highly oriented pyrolytic graphite (HOPG) by laser-driven compression with $2 \times 10^{15}\ \text{W cm}^{-2}$, but they did not consider the nanocrystallization of ceramics.

Here, shocks driven by a femtosecond laser are applied on single crystal YSZ ceramics, and we report the crystal orientation, spallation structure, polycrystallization, and outside and inside structure, as well as the residual stress. Experimental results provide the nanocrystallization of YSZ ceramics with ultra-intense laser-driven shock waves.

2. Experimental procedure

Figure 1(a) shows the laser system HAMA [10]. The seed is a titanium:sapphire laser BEAT [11–13]. The output beam from the BEAT is pumped by the second harmonics of a KURE-1 [14] (with 4.4 J of energy, a wavelength of $2\omega_0 = 527\ \text{nm}$, and a width of 15 ns). Combined four-grating pulse compresses the output to a femtosecond beam (an ultra-intense laser with 0.84 J, $\omega = 820\ \text{nm}$, 110 fs), which is divided into two beams by a beam splitter in the compressor chamber. The two laser beams are then focused in a diameter of $65\ \mu\text{m}$ on the YSZ with a pair of off-axial parabolic mirrors (OAP 1 and OAP 2) set in a vacuum chamber. As shown in figure 1(b), a single shot of an ultra-intense laser beams counter-irradiated the

YSZ. The shape of the YSZ sample with a 11.5 mol% Y_2O_3 cubic crystal was $10\ \text{mm} \times 10\ \text{mm}$ square in a (100) crystal orientation. The ambient pressure was $\sim 10^{-3}\ \text{Pa}$. The irradiated laser conditions are summarized in table 1.

We simultaneously irradiated a 0.5 mm-thick YSZ plate on both sides with two counter beams from an ultra-intense laser with 0.4 J of energy, a pulse width of 110 fs, and peak intensity of $1.15 \times 10^{17}\ \text{W cm}^{-2}$. The focal intensity is one or two order higher than that of conventional laser-driven shock compression.

We analyzed the crystalline structure of the YSZ using the beam line of the Aichi Synchrotron Radiation Center. We used the BL5S2 beam line (energy range = 5–23 keV (0.25–0.05 nm), beam size is 0.5 mm in vertical and 0.5 mm in horizontal, and resolution $(E/\Delta E) = 7000$ at 12 keV) for crystalline analysis by x-ray diffraction. This beam line is attached to the Debye–Scherrer camera ($R = 286\ \text{mm}$), the imaging plate (IP BAS-MS, 200 mm-width \times 400 mm-length, FUJIFILM) and the imaging plate reader (RAXIS-DS3C, Rigaku). The irradiation angle to the YSZ was $10.000 \pm 0.004^\circ$ in a grazing incidence, the beam size was $0.6\ \text{mm} \times 0.5\ \text{mm}$, the energy was 12.4 keV, the irradiation time was 10 min, and the skin depth of the x-ray at this time was $10.1\ \mu\text{m}$. The sample attachment error in the setup was 0.1 mm or less.

We also analyzed the irradiated YSZ's surfaces and cross-sections using the following techniques: electron backscatter diffraction (EBSD), x-ray diffraction (XRD), as well as a scanning electron microscope (SEM), and a scanning transmission electron

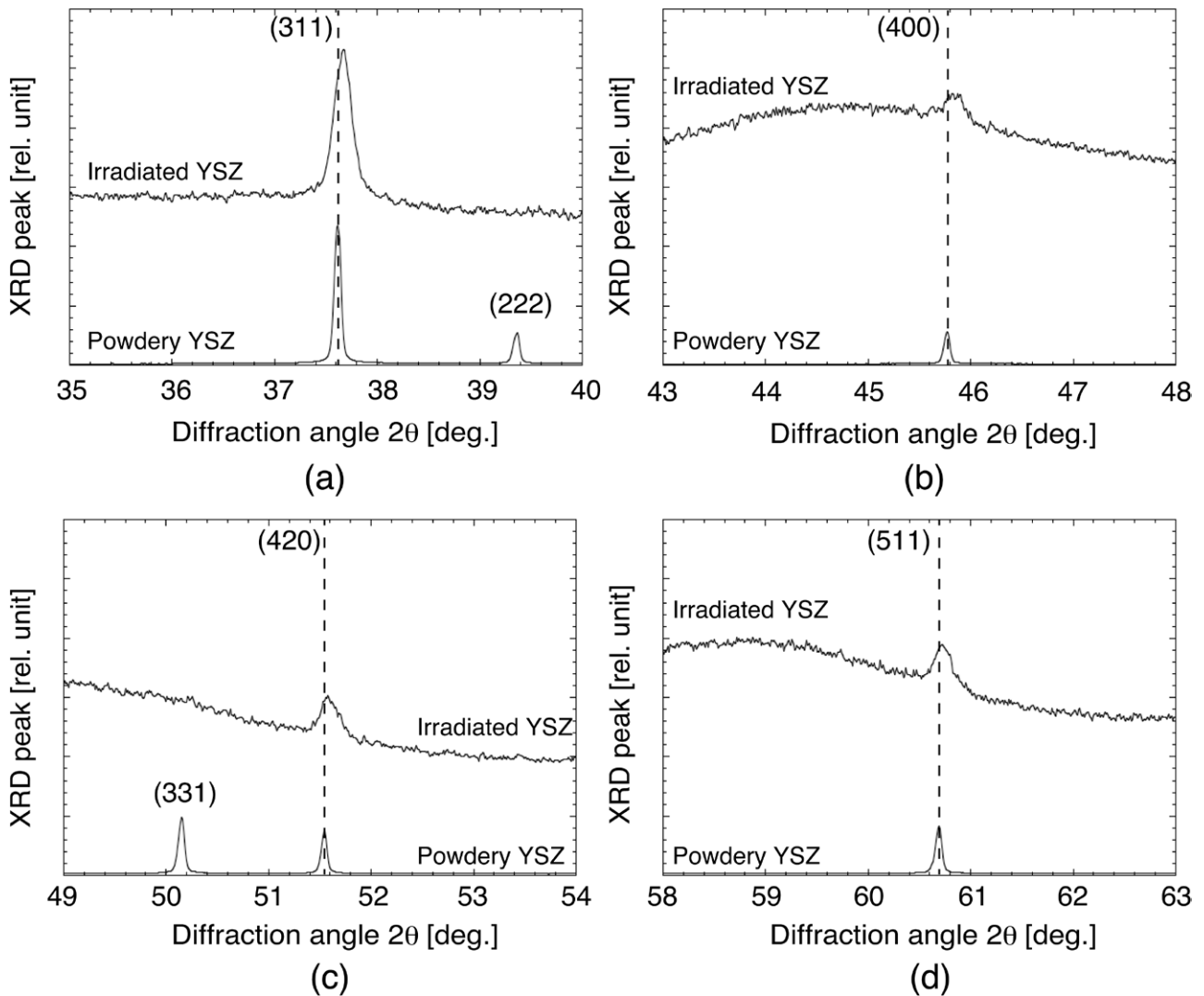


Figure 3. Observation results from the x-ray diffraction (XRD) one-dimensional profile from irradiated and nonirradiated powdery YSZ. (a) Lattice plane (311), (b) Lattice plane (400), (c) Lattice plane (420), and (d) Lattice plane (511). All figures demonstrate that the single-crystal YSZ is changed to a polycrystalline state by ultra-intense laser.

microscope (STEM). We used the EBSD technique, the SEM (Ultra 55, Carl Zeiss), and the STEM (EM-002BF, Topcon) to analyze the surface and inside the counter-irradiated YSZ.

3. Results and discussion

Figure 2(a) shows the cross-section image of SEM. We broke the sample along the cross-section of the sample, a big crack is seen on the outside of the laser irradiation area. A small crack also is seen to propagate in the laser irradiation area. It seems that a small crack in the laser irradiation area could not endure the impact by laser-driven shock wave and so it is made.

In figure 2(b), the crystal orientations (001) and (101) appear from the surface to a depth of 12 μm of the first layer, showing that the single crystal YSZ of the first layer was changed to a polycrystalline state by ultra-intense laser irradiation. Figure 2(c) shows that in the second layer from a depth of 12 to 28 μm , the few tens nanometer grains seem to appear by a laser-driven shock wave. In the third layer,

from a depth of 28 to 96 μm the size of the crystal grains is larger than that in the second layer. Since the area deeper than 96 μm remains as a single crystal YSZ, the laser-driven shock wave must reach up to the third layer. We also determined the penetration depth of the shock wave to be 150 μm or less, the shock waves from both sides do not seem to interact with each other.

Figures 3(a)–(d) show XRD results from a diffraction angle of 35°–63°. In all figures, the XRD peaks indicate that the single-crystal YSZ has become polycrystalline by the ultra-intense laser. We have based on the nonirradiated powdery YSZ peaks. Note that the peaks from lattice planes (311), (400), (420), and (511) have shifted to higher diffraction angles, respectively.

Assuming that a change of lattice spacing is the amount of deformation, we estimated the residual stress along beam propagation direction from an XRD profile. The residual stress estimated the compressive stress with $-110 \sim -310$ MPa by using Hooke's law. The XRD analysis 100 days after illumination leads us to conclude that the residual stresses have been

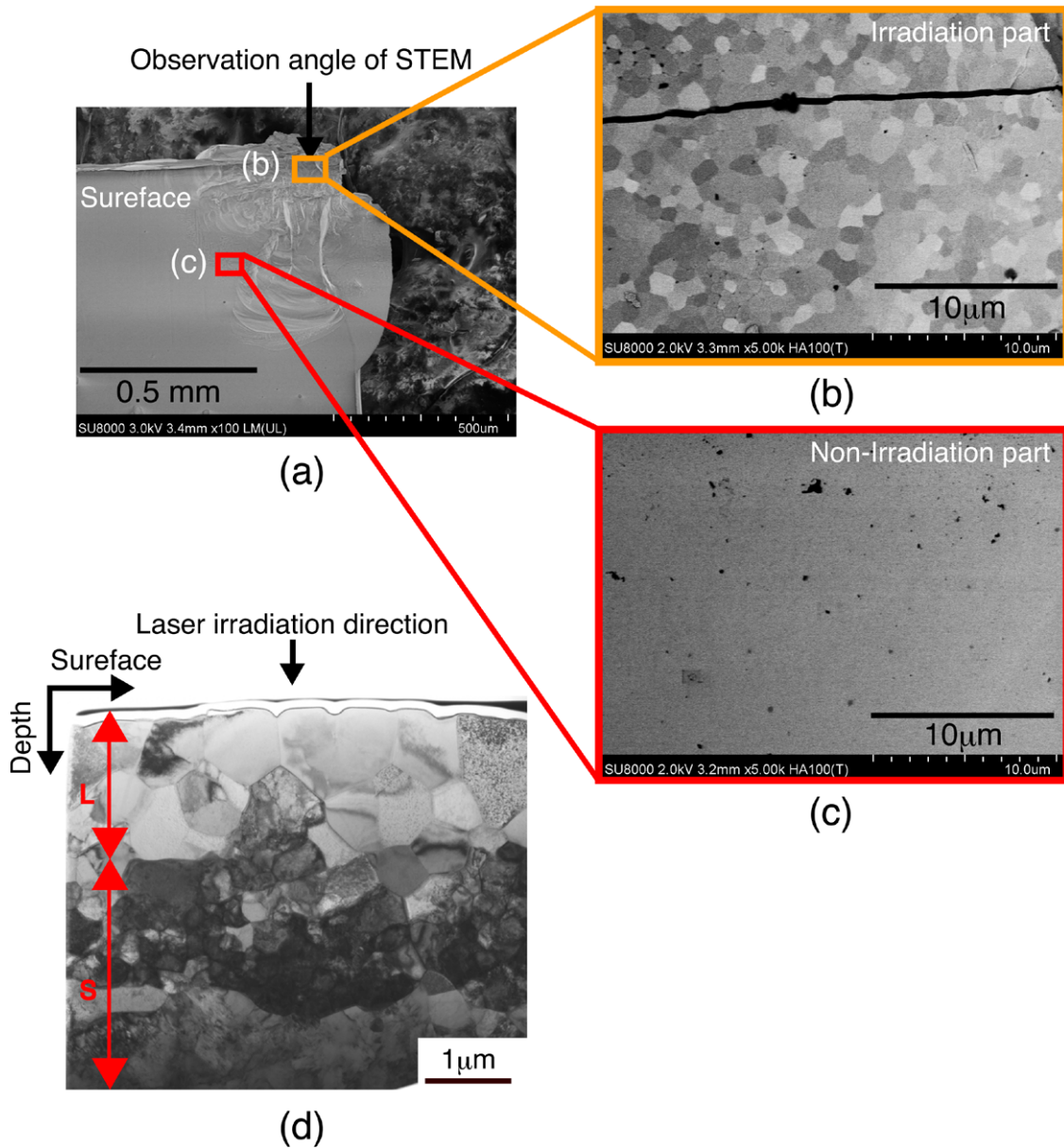


Figure 4. Observation results of the irradiated YSZ (a) on the OAP 1 side with an SEM, (b) the enlarged view of a reflection electron image at the irradiation area in (a), (c) the enlarged view of a reflection electron image at the nonirradiation part in (a), and (d) the cross-section of the irradiated area observed with a STEM. L indicates the large grains layer. S indicates the small grains layer. These figures show that the irradiated area changed from single crystal YSZ to polycrystalline YSZ.

frozen for more than 100 days in the film thickness direction. And we estimated that plastic deformation has happened in the sample due to ultra-intense laser irradiation.

To see the grain size variations precisely, we investigated the first layer using an SEM, as shown in figure 4(a). Figures 4(b) and (c) show expanded views of areas in figure 4(a). The irradiated area in figure 4(b) shows multiple crystal grains, which we compared with the nonirradiated area in figure 4(c). Thus, we can conclude that the ultra-intense laser modified the surface of a single crystal to a polycrystalline state. The crystal grain size in figure 4(b) is approximately 1 μm.

Using the STEM, we more precisely analyzed the cross-section of the first layer. From the surface to 4 μm in depth, we observed a double-layered polycrystalline structure, as shown

in figure 4(d). Furthermore, from the surface to a depth of 1.7 μm (L layer) the crystal grain size is approximately 1 μm, and from 1.7 μm to 4 μm in depth (S layer), the crystal grain size is less than 200 nm. The size of the crystal grains in the L layer agrees with the SEM observation results (see figure 4(b)).

We found for the first time nanocrystallization inside a single crystal YSZ of ceramics. Typically, such a nanocrystallization was seen in a metal dislocation. We are assuming it is a nanocrystallization of YSZ and that the slipping along the lattice plane is caused by a laser-driven shock compression.

Our experimentally observed spatial profile of the grain size can be explained by the model of shock and heat waves described below. When an ultra-intense laser irradiates a surface of the crystal, the surface is pushed by the high pressure

driven by the ponderomotive force of the laser [15, 16]. We can estimate the pressure P by;

$$P = (1 + \eta) \frac{I_L}{c}, \quad (1)$$

where η is the reflectivity of the laser at the surface, which is nearly 1 for the short pulse of 110 fs duration. I_L and c are, respectively, the laser intensity and the speed of light. With a laser intensity of $1.15 \times 10^{17} \text{ W cm}^{-2}$ used in this experiment, P is about $7.6 \times 10^{12} \text{ Pa}$.

When this high pressure is applied on the surface of single crystal YSZ, a shock wave starts from the laser irradiation spot in the material. As the shock wave front passes, polycrystallization and micronization occur in the material. As the shock propagates deeper into the material, the pressure behind the shock wave front decreases. After propagating several times the laser spot size, it becomes weak and polycrystallization and micronization stop. Therefore, we do not find polycrystallized material in the deep part. At the same time, near the surface, the laser irradiation creates a high temperature plasma plume around the irradiating laser spot. The thermal conduction from this plume causes the polycrystallized material to melt and adhere with each other crystals, forming grains larger than polycrystal¹. However, as the high temperature plume expands towards the vacuum space and the temperature lowers after laser irradiation, this melting near the surface stops. As the result, the grain size near the surface is larger than that in the deeper part. This increase of the grain size near the surface will be larger, if the thermal conductive heat load is larger.

4. Summary

The ultra-intense laser irradiation changed the surface of the single crystal YSZ to a multilayered polycrystalline state with nanometer-sized grains to a depth of 100 μm . The laser intensity is three order higher than that in the conventional laser shock compression. The laser-driven shock wave, which penetrated 96 μm into the crystal, caused it to form a four-layered structure (the first layer from the surface to 12 μm , the second from 12 to 28 μm , the third from 28 to 96 μm , and the fourth from 96 to 130 μm). The grain size of the first layer was 1 μm , while that of the second layer was broken into a few tens of nanometers. The grain size of the third layer was a few hundred of nanometers to a few ten of micrometers. The area deeper than 96 μm remained as a single crystal. The first layer details show that the grain sizes from the surface to 4 μm in depth were separated by 1 and 0.2 μm , respectively. The plasma heat wave might remelt the first layer, resulting in the grain size becoming larger than that in the second one. The

XRD peak shifts suggest that the residual stresses are frozen in the film thickness direction due to the effects of surface polycrystallization. Our experimentally observed spatial profile of the grain size can be explained by this shock and heat waves model.

The polycrystallization of ceramics is useful for making ceramics tougher, because the ceramic material is brittle and easily destroyed by impact or thermal shock. If nano crystallization overcomes such defects and increases the toughness of ceramics with respect to fracture, ceramics could be used much more widely by industries.

Acknowledgments

We are deeply grateful to Dr Y Takeuchi and the KURE-1 laser technical crew of Hamamatsu Photonics KK for their exceptional support while performing these experiments. We acknowledge Ms M Ito of Toyota Motor Corporation for EBSD, SEM, and STEM analysis support. We are grateful to Dr M Yoshimura and Mr Y Nakanishi of Aichi Science and Technology Foundation for valuable discussions of x-ray diffraction measurement. Thanks to Mrs S Suita of The Graduate School for the Creation of New Photonics Industries for experiment preparation support.

References

- [1] Sato K 2011 *J. Plasma Fusion Res.* **87** 36–41
- [2] Ueda T, Umeda M, Okawa H and Takahashi S 2011 *IOP Conf. Ser.: Mater. Sci. Eng.* **18** 212012
- [3] Cuq-Lelandais J P, Boustie M, Berthe L, de Rességuier T, Combis P, Colombier J P, Nivard M and Claverie A 2009 *J. Phys. D: Appl. Phys.* **42** 065402
- [4] Tsujino M, Sano T, Ozaki N, Sakata O, Okoshi M, Inoue N, Kodama R and Hirose A 2008 *Rev. Laser Eng. (APLS)* **36** 1218–21
- [5] Tsujino M, Sano T, Ogura T, Okoshi M, Inoue N, Ozaki N, Kodama R, Kobayashi K F and Hirose A 2012 *Appl. Phys. Express* **5** 022703
- [6] Matsuda T, Sano T, Arakawa K, Sakata O, Tajiri H and Hirose A 2014 *Appl. Phys. Express* **7** 122704
- [7] Matsuda T, Sano T, Arakawa K and Hirose A 2014 *Appl. Phys. Lett.* **105** 021902
- [8] Sano T, Takahashi K, Sakata O, Okoshi M, Inoue N, Kobayashi K F and Hirose A 2009 *J. Phys.: Conf. Ser.* **165** 012019
- [9] Sano T and Hirose A 2014 *Rev. Laser Eng.* **42** 452–6
- [10] Mori *et al* 2013 *Nucl. Fusion* **53** 073011
- [11] Mori Y, Fukumochi S, Hama Y, Sentoku Y and Kitagawa Y 2007 *Int. J. Mod. Phys. B* **21** 572
- [12] Mori Y and Kitagawa Y 2012 *Phys. Plasmas* **19** 053106
- [13] Mori Y and Kitagawa Y 2013 *Appl. Phys.* **110** 57–64
- [14] Sekine T *et al* 2010 *Opt. Express* **18** 13927–34
- [15] Wilks S C, Kruer W L, Tabak M and Langdon A B 1992 *Phys. Rev. Lett.* **69** 1383
- [16] Sentoku Y, Kruer W, Matsuoka M and Pukhov A 2006 *Fusion Sci. Technol.* **49** 278

¹ Private communication with the co-author Atsushi Sunahara on his STAR ID hydrocode including radiation transport, to be published elsewhere.